Original Article
J. Korean Wood Sci. Technol. 2024, 52(1): 47-57
https://doi.org/10.5658/WOOD.2024.52.1.47

Journal of the Korean Wood Science and Technology
pISSN: 1017-0715 eISSN: 2233-7180
http://www.woodj.org

Fixed Bed Drying of Sugarcane Bagasse Using Solar Energy

Hyoung-Woo LEE[1,†] · Hyun-Ook KIM[2] · Dong-Hoon LEE[2] · Don-Ha CHOI[3] · Seung-Gyu KIM[1]

ABSTRACT

Solar energy is one of the most promising options for renewable energy and biomass is one of them. One of the main biomass sources, sugarcane bagasse, is produced annually in more than hundreds of nations worldwide exceeding 4.25 billion tons. To dry a 900-mm deep fixed bed of wet sugarcane bagasse, a solar air heater with a collector area of 2 m^2 was installed. Between October 10th to 19th in Gwangju, South Korea, a 9-day drying period, the solar collector received a total of 496,145 kJ of solar radiation. During this time, 54.5 kg of water was extracted from 133 kg of wet sugarcane bagasse (average green moisture content of 47.6%$_{w.b.}$). The estimated net heat from the evaporation of water removed during the dying period accounted for approximately 27% of the total solar radiation on the solar collector.

Keywords: drying, solar drying, sugarcane bagasse, biomass, solar energy

1. INTRODUCTION

Lignocellulosic materials are important and abundantly available biomass feedstock for the fuels (Cahyani *et al*., 2023; Kim *et al*., 2023a, 2023b; Pari *et al*., 2023; Sutapa and Hidyatullah, 2023), the platform chemicals (Jung *et al*., 2022; Myeong *et al*., 2023), the construction materials (Aisyadea *et al*., 2023; Dungani *et al*., 2022; Jang, 2022; Setyayunita *et al*., 2022) and the nanocomposite materials (Shrestha, 2022).

Global sugar production in 2019 accounts for approximately 80% sugarcane and 20% sugar beet (Mohammadi *et al*., 2020). Over 1.7 billion tons of sugarcane are produced globally in more than hundred countries (Arshad and Ahmed, 2016). Each metric ton of sugarcane produces approximately 250 kg of bagasse (Salehi *et al*., 2013).

Bagasse is the main byproduct from the cane sugar manufacturing process. Bagasse is a fibrous material obtained after the sugar juice is leached from the sugarcane. The moisture content of the green sugarcane bagasse is approximately 50% upon leaving the mill. Bagasse is typically burned to produce steam and electricity (Akomo, 2016). Iswanto *et al*. (2020) and Jamaludin *et al*. (2020) used sugarcane bagasse as raw material to produce particleboard. Currently, trend of

Date Received October 31, 2023; Date Revised November 28, 2023; Date Accepted December 5, 2023; Published January 25, 2024
[1] College of Agriculture and Life Science, Chonnam National University, Gwangju 61186, Korea
[2] Department of Environmental Engineering, University of Seoul, Seoul 02504, Korea
[3] Korea Forestry Promotion Institute, Seoul 07570, Korea
[†] Corresponding author: Hyoung-Woo LEE (e-mail: dryingeng@daum.net, https://orcid.org/0000-0001-6451-325X)

using non-woody biomass as an environmentally friendly renewable biobased product is increasing (Zendrato *et al*., 2021). Bioethanol, a fuel additive for transportation, is produced mainly by using first generation biomass such as corn and sugarcane (Heo and Choi, 2017). Fatriasari *et al*. (2020) improved hydrolysis of sugarcane trash for the production of fermentable sugar by adding surfactants.

According to Naeem (2019), the bagasse power plants reduce carbon emissions by replacing electricity produced from fossil fuels and avoiding the disposal of unused bagasse which generates methane emissions on decomposition. The gross calorific value of ash-free and moisture-free sugarcane bagasse is 19.6 MJ/kg. However, the net calorific value (NCV) at moisture content of 50% becomes 7.9 MJ/kg (Don *et al*., 1977). Therefore, the reduction of moisture by drying can increase the NCV of bagasse and the efficiency of the heat generation system using bagasse as fuel.

Performance of the drying process depends largely on the effective use of thermal energy. The sun is the largest available carbon-free energy source available to mankind. The first use of solar energy for drying purposes dates back to 8,000 B.C. However, the conventional drying industry started around the 18^{th} century (Belessiotis and Delyannis, 2011). Sustainable systems based on solar energy are playing an important role in the drying of biomass and agro-products because of their low operating costs. Abdel-Rehim and Nagib (2007) investigated the solar drying characteristics of bagasse pulp using natural and forced air convection. The results indicate that forced air convection saved the drying time. Krog (2018) reported that bagasse fuel consumption can be reduced by 5% if only exhaust steam is included in the bagasse drying process, but it can be reduced by 7.05% if the solar system is used.

To obtain the desired quality and performance. solar systems must be properly designed and scaled to meet the requirements of specific biomass and environments. This study aims to manufacture an indirect-type solar dryer with an external solar collector as an air heater in order to verify the possibility of solar drying of sugarcane bagasse.

2. MATERIALS and METHODS

2.1. Material preparation

Milled sugarcane (*Saccharum officinarum* L.) bagasse imported from Vietnam was the biomass used in this study. Moisture analyzer (ML-50, A&D, Tokyo, Japan) was used to determine the moisture content of the bagasse. The average moisture content of the seven bagasse samples was 10.7%w.b. (SD 1.4%w.b.).

Tap water was added to the bagasse during agitation in the industrial mixer to simulate the green state at moisture content of approximately 50%. A total of 133 kg of the wet bagasse (average moisture content 47.6%w.b.) was prepared and loaded into the drying chamber to attain the final bed depth of approximately 900 mm.

2.2. Determination of particle size

A representative sample of 50 g of sugarcane bagasse was fractionated using sieving techniques to determine the distribution of particle sizes. The equipment used was a CISA electromagnetic sieve shaker model RP 200N, with a sieving time of 10 min. 7 Screens with orifices of 9.50, 4.00, 2.00, 1.00, 0.60, 0.212, and 0.18 mm and the bottom were used. An additional sieving time over the 10 min had no effect on the particle mass fraction on each sieve. The mass fraction retained on each sieve was weighed using a CAS digital electronic balance model MWII-300H, with an accuracy of 0.01 g. The same experiment was repeated 3 times and the average value was adopted as the result. In 1926 Sauter introduced a method for calculating the mean diameter

of a collection of different-size objects by considering both the volume and surface area (Kowalczuk and Drzymala, 2016). The Sauter mean diameter concept has been widely used to determine the average size of particles. In this study the Sauter mean diameter of the raw sugarcane bagasse particles was calculated using Equations (1) and (2), as proposed by Kunii and Levenspiel (1991) and Geldart (1986);

$$\bar{d}_p = \frac{1}{\sum_{i=1}^{n}(\frac{x_i}{d_{pi}})} \quad (1)$$

$$\bar{d}_{pi} = \left[\frac{(x_i^2 + x_{i+1}^2)\times(x_i + x_{i+1})}{4}\right]^{0.33} \quad (2)$$

$\bar{d}_p$: Sauter mean diameter.

x_i: Mass fraction of particles with an average diameter d_{pi}.

d_{pi}: Mean value between the aperture of the sieve that allowed that fraction to pass through, and that of the sieve that retained the fraction.

2.3. Drying chamber

Agro-industrial organic solid wastes such as a sugarcane bagasse are generally dried as a form of the fixed bed type piles. Therefore, the drying chamber was designed to simulate the fixed bed in this study.

The drying chamber had a square cross section, 1,000 mm on each side, a height of 1,200 mm, and a total internal volume of 1.2 m^3 (Fig. 1). The drying chamber's walls, top, and bottom were insulated with 100 mm–thick fiberglass. The bottom plate of the drying chamber was perforated with holes (diameter 5 mm) to distribute the drying air from the blower. The open area ratio of the bottom plate was approximately 33%. The height of the air plenum chamber under the bottom plate is 100 mm. The drying air inlet and outlet were located at the top and bottom of the drying chamber, respectively. Therefore, drying air flowed from the bottom to the top of the sugarcane bagasse bed.

Thermocouples were used to measure temperatures at the drying chamber's air-inlet and -outlet of drying chamber, and at three locations in the bed (230, 560 and 790 mm in height from the bottom plate). The bagasse bed in the drying chamber had a height of 900 mm and

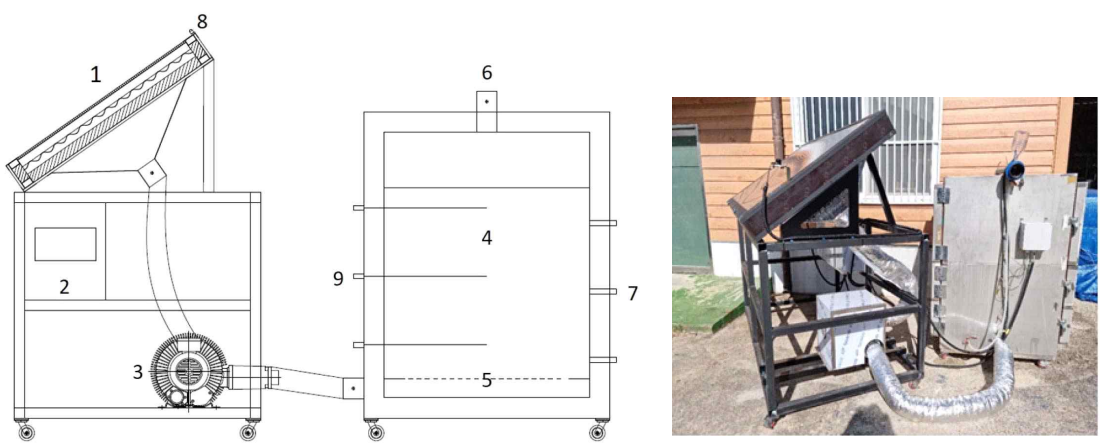

Fig. 1. Schematics of solar dryer. 1: solar air heater, 2: data logger, 3: blower, 4: drying chamber, 5: perforated plate, 6: air outlet, 7: three sampling pockets, 8: pyranometer, and 9: three temperature sensors.

a 300 mm high freeboard.

At heights of 200, 400, 600, and 800 mm from the bottom, three holes with a diameter of 30 mm were drilled on the drying chamber's side wall to obtain four wet-based moisture content ($MC_{w.b.}$) samples. The layers at 200, 400, 600, and 800 mm from the bottom were labeled as the 1st, 2nd, 3rd, and 4th layers, respectively, for convenience. To collect these samples four times a day (9, 12, 15 & 18 O'clock) during drying, a pocket sampler (diameter 25 mm, length 540 mm) was used.

2.4. Solar air heater

The external dimensions of solar air heater were 2,126 mm-long, 1,126 mm-wide and 157 mm-thick (Fig. 2). The solar collector's dimensions were 2.0 m in length and 1.0 m in width, giving a total collector area of 2 m^2. The solar air heater comprised a corrugated galvanized steel sheet (0.5 × 1,000 × 2,000 mm) coated with matt black paint as an absorber plate and a double-layered transparent polycarbonate panel (10 × 1,000 × 2,000 mm) for glazing. A 50-mm-thick high-density styrofoam was used as insulation on the exterior of the solar air heater. The rear plate of the solar air heater and its four sidewalls were made of 9-mm-thick water-resistant plywood. The diameter of the air inlet and outlet ducts was 100 mm. The distance between the glazing panel and the absorber plate was 40 mm. Ambient air flows under the absorber plate and the sectional area of the air passage was calculated as 0.0335 m^2. To maximize the average daily solar insolation, a solar air heater was installed at an angle of 35° south -approximately the same latitude as that in Gwangju, Korea. A pyranometer (SP-214-SS, Apogee Instruments, Logan, UT, USA) installed horizontally on the solar air heater was used to monitor the intensity of solar radiation.

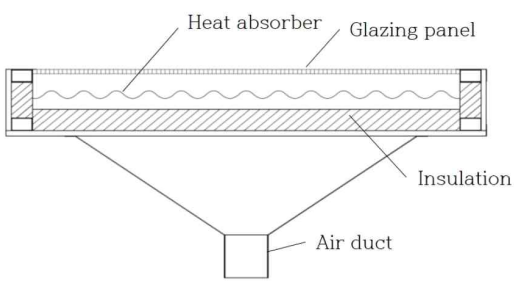

Fig. 2. Sectional side view of the solar air heater.

2.5. Air flow rate

A high-pressure explosion-proof blower (ExB-TBS/T-301S, INNO TECH, Cheongju, Korea) with a motor power of 0.75 kW, a maximum static pressure of 2,019 Pa, and a maximum volumetric air flow rate of 27 m^3/min provided the drying chamber with drying air. The blower is controlled by a variable-frequency drive and is coupled to the solar air heater's air outlet duct. The blower forces ambient air into the solar air heater, which then supplies heated air to the drying chamber.

Air velocity was measured by pitot tube type anemometer (AF121B, M. Paul, Oviedo, FL, USA) inserted into the duct between the blower and drying chamber. The average maximum volumetric air flow rate was estimated as 7.2 m^3/min. Volumetric air flow rate of a blower decreases as the pressure drop increases. Based on the blower performance data provided by this blower manufacturer the total pressure drop across the whole solar drying system with empty drying chamber was estimated as 1,650 Pa at the volumetric air flow rate of 7.2 m^3/min.

The differential pressure sensor (TESTO 510, Testo AG, Titisee-Neustadt, Germany) measured the pressure drops throughout the drying process. At the maximum volumetric air flow rate, the estimated pressure drops across the drying chamber were 55 Pa when empty and 251 Pa when loaded with a 900-mm-deep wet bagasse bed. The pressure drop induced by the 900 mm-deep wet bagasse bed was calculated as 196 Pa. Therefore, it was determined that the total pressure drop across the

entire solar drying system with a 900-mm-deep wet bagasse bed was approximately 1,846 Pa. Based on the blower performance data, the volumetric air flow rate into the wet bagasse bed was estimated as 3.9 m^3/min.

2.6. Determination of solar dryer thermal efficiency

The instantaneous thermal efficiency of the solar air heater can be estimated using Equation (3). Given that F_R, τ, α, U_L are constants for a given collector and flow rate, the efficiency is a linear function of the following three parameters that define the operating condition: solar irradiance (I), fluid inlet temperature (T_i), and ambient air temperature (T_a) (Struckmann, 2008).

$$\eta = \frac{F_R A[I\tau\alpha - U_L(T_i - T_a)]}{AI} = F_R\tau\alpha - F_R U_L(T_i - T_a)/I \quad (3)$$

η: Collector thermal efficiency.
F_R: Collector heat removal factor.
A: Collector area (m^2).
τ: Transmission coefficient of glazing.
α: Absorption coefficient of plate.
U_L: Overall collector heat loss coefficient (W/m^2).
T_i: Inlet fluid temperature (℃).
T_a: Ambient temperature (℃).
I: Intensity of solar radiation (W/m^2).

The efficiency of a solar collector is defined as the ratio of the amount of useful heat collected to the total amount of radiation striking the collector surface during any period.

$$\eta = \frac{Q_u}{AI} = \frac{\dot{m}C_p(T_o - T_i)}{AI} \quad (4)$$

Q_u: Useful heat collected by the solar collector (W).
A: Collector area (m^2).
I: Intensity of solar radiation (W/m^2).
$\dot{m}$: Air mass flow rate (kg/s).
C_P: Specific heat of air at constant pressure (J/kg K).

The thermal efficiency increases with increasing mass flow rate. Increasing the solar radiation intensity leads to an increase in the air temperature and thermal efficiency (Chabane *et al.*, 2013; Saha, 2020).

The thermal properties of air are considered as variables according to the following expressions (Tiwari, 2002), where the fluid temperature is measured in Celsius:

$$C_p' = 999.2 + 0.143T_a + 1.101\times10^{-4}T_a^2 - 6.7581\times10^{-8}T_a^3 \quad (5)$$

$$\rho_a = \frac{353.44}{273 + T_a} \quad (6)$$

ρ_a: Density of air (kg/m^3).

The net heat efficiency of the drying chamber is defined as the ratio of the net heat used to evaporate water in sugarcane bagasse to the total useful heat supplied to the drying chamber by the solar air heater. Net heat required to vaporize water is given to be approximately 2,453 kJ/kg of water at 20℃ and 1 atm (Osborne *et al.*, 1939).

$$\eta = \frac{\lambda_{ev} m_{ew}}{H_u} \times 100(\%) \quad (7)$$

η: Net heat efficiency of the drying chamber (%).
λ_{ev}: Latent heat of evaporation of water (kJ/kg).
m_{ew}: Total water removal (kg).
H_u: Total useful heat supplied to drying chamber by solar collector (kJ).

3. RESULTS and DISCUSSION

3.1. Particle size analysis

The raw bagasse was subjected to a previous process of milling in two stages to reduce its size and produce a fine powder with particle sizes ranging from 0.063–0.6 mm (El-Sayed and Mostafa, 2014).

The bagasse analysis showed that the mass of the particles retained in four sieves with apertures of 2.0, 1.0, 0.60, and 0.21 mm was 89.72% of the total particle mass (Fig. 3). The mass fraction of particles smaller than 0.21 mm is 8.90% of the total particle mass. The Sauter diameter $\bar{d}_p$ was estimated as 0.354 mm using Equation (1) (Table 1).

The standard separation method using a vibrating sieve shaker assumes homogeneous, uniformly shaped particles. According to Lee and Eom (2021), an air classifier can be an appropriate solution for separating particles with needle-like shapes, such as sugarcane bagasse.

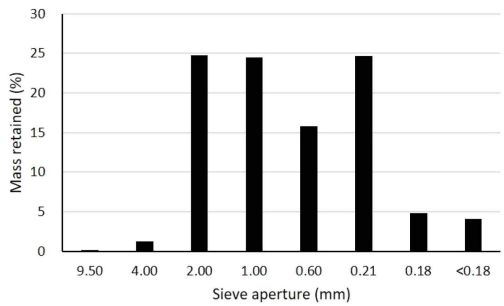

Fig. 3. Particle size distribution of sugarcane bagasse.

3.2. Solar radiation and temperature profiles

Fig. 4 shows the variations in solar radiation (SI) and drying chamber inlet air temperature (Ti) throughout the solar drying of sugarcane bagasse from October 10th to 19th. As solar radiation intensity increased, the temperature of air supplied from the solar air heater also increased. During this drying period, the inlet air reached a maximum temperature of 46.1℃, with a temperature difference of 21.2℃ between the ambient and inlet air at an average air mass flow rate of 0.078 kg/s.

The maximum solar radiation, recorded from October 10th to 19th was 1,686 W/m^2. During the drying period, the total solar radiation on the 2 m^2 solar collector was 496,145 kJ.

Fig. 5 shows the temperature profiles of the bed in the drying chamber. As expected, the temperature profiles at 3 points in the bed followed that of the inlet air. The sugarcane bagasse in the bed uses the heat from the warm inlet air as both sensible heat to raise the temperature and latent heat to evaporate water. During the

Table 1. Particle size analysis results of milled sugarcane bagasse

Sieve aperture size (mm)	Weight fraction (x_i)	d_{pi} (mm)	$\sum_{i=1}^{n}(\frac{x_i}{d_{pi}})$
9.5	0.0017	6.967	0.0002
4.0	0.0121	3.072	0.0039
2.0	0.2479	1.547	0.1603
1.0	0.2451	0.818	0.2996
0.6	0.1580	0.438	0.3604
0.212	0.2463	0.200	1.2336
0.180	0.0885	0.116	0.7680
Bottom	0.0405		
Sum	1.0000		2.8260

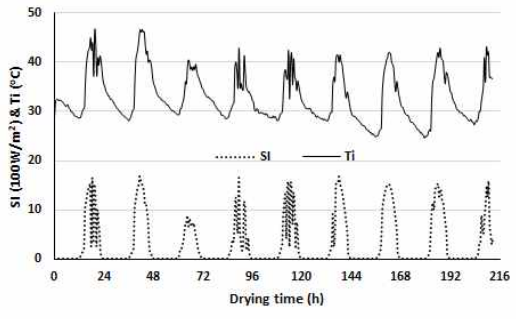

Fig. 4. Changes of solar insolation (SI) and drying chamber inlet air temperature (Ti) during solar drying of sugarcane bagasse from October 10th to 19th.

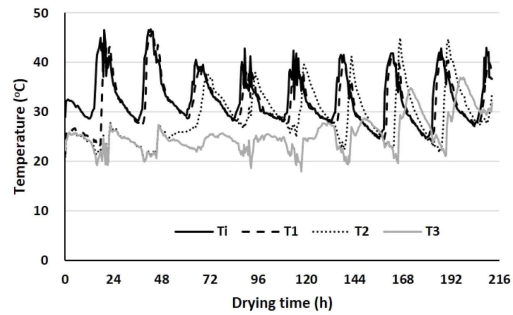

Fig. 5. Temperature profiles in drying chamber during solar drying of sugarcane bagasse from October 10th to 19th. Ti: inlet air temperature, T1: temperature at the height of 230 mm in the bed, T2: temperature at the height of 560 mm in the bed, and T3: temperature at the height of 790 mm in the bed.

early stages of drying, much of the latent heat is consumed. However, as drying time elapses, the bed's moisture content decreases and sensible heat consumption increases significantly. Therefore, the bed's temperature became closer to that of the inlet air. The temperature at a height of 560 mm in the bed (T2) appeared to be the highest in the bed during the last stage of this drying period (after 168 hours). This phenomenon may be an indication of the potential for self-heating due to the fermentation of bagasse in the middle of the bed.

3.3. Drying rate

On October 10th, 2023, 900-mm wet bagasse was subjected to solar drying. The bed's 1st layer dried very quickly. In just one day, it dried from 43.9% $MC_{w.b.}$ to 9.4% $MC_{w.b.}$. However, it took 5 days for the 2nd layer of the bed to dry enough to reach an $MC_{w.b.}$ of approximately 10%. The bed's 3rd and 4th layers required between 6 and 9 days, respectively, to reach approximately 10% $MC_{w.b.}$ (Fig. 5). The drying rates of the bed's layer are shown in Table 2.

Assuming that the desired moisture content of bagasse post-drying is less than 30%$_{w.b.}$, it will take approximately 7 days for the top layer of the bagasse bed in this solar drying system to attain its ultimate moisture content, while the moisture contents of the layers below it have already decreased to 10%. If the drying chamber's bottom area is increased, the bagasse bed's depth with the same total volume of 0.9 m^3 can be decreased to approximately 450 mm. The top layer of the bagasse bed would be the 2nd layer. After that, the top layer should only take 3 days to dry and attain the desired final moisture content of 30%$_{w.b.}$. However, for a given dryer capacity, the area required for solar dryer installation will increase as the bed depth decreases.

Without increasing the drying chamber's base area, installing agitating devices inside the drying chamber can greatly speed up the drying process and enhance the homogeneity of the final moisture content in the bagasse bed. A semi-continuous type bed dryer is an additional option. When the bottom layer of the bagasse bed in this dryer reaches the desired moisture content, it is discharged from the drying chamber and replaced with the same volume of wet bagasse as the top layer. This process will be repeated until the total production goal is attained.

Table 2. Drying rates of each part of the sugarcane bagasse bed

Layer	1st	2nd	3rd	4th
Initial $MC_{w.b.}$ (%)	43.9	45.1	47.6	47.6
Final $MC_{w.b.}$ (%)	8.6	8.9	9	10.5
Drying time to 10% $MC_{w.b.}$ (days)	1	5	6	9
Drying rate to 10% $MC_{w.b.}$ (%/day)	34.5	7.0	6.3	4.2

3.4. Thermal efficiency

After 9 days of drying, the total weight of the bed reduced from 132.9 kg to 78.4 kg. For 9 days, 54.5 kg of water was extracted. The average water removal rate can be estimated to be 12.1 kg/day.

During the drying period, the thermal efficiency of the solar air heater was measured for 6 h, from 10 am to 3 pm, on each sunny day. During the 34 h of this evaluation period, the average solar radiation was 2,634 W, and the average usable heat collected was calculated as 1,350 W. Therefore, the thermal efficiency of the solar air heater can be estimated as 51.3% by Equation (4). According to Rasheed *et al*. (2023), in May 2022, in Baghdad, Iraq (33.333° latitude), the thermal efficiency of the single-pass solar air heater with flat absorber ranged from 42.5% to 68.1% (average 55.3%).

To vaporize 54.5 kg of water (2,453 kJ/kg of evaporated water), a total heat of vaporization of about 133,689 kJ is required. Krog (2018) stated that the thermal requirements for drying sugarcane bagasse from 45%$_{w.b.}$ to 10%$_{w.b.}$ moisture content using industrial-scale rotary dryers and pneumatic dryers are 3,000−4,000 and 2,700−2,800 kJ/kg of evaporated water, respectively. The thermal requirements of these dryers are greater than those of this solar dryer. The much higher drying temperatures at which Industrial-scale dryers operate seem to induce higher heat losses than solar dryers.

This heat is equivalent to approximately 27% of the estimated 496,145 kJ of solar radiation that the solar collector received throughout the drying period. The heat input from the solar air heater was calculated as 254,522 kJ (= 496,145 × 51.3%). Therefore, the net thermal efficiency of the drying chamber can be calculated as 52.5% using Equation (7). However, the calculation of these thermal efficiencies did not account for the heat used to increase the temperature of the sugarcane bagasse bed or the electrical energy input from the blower.

4. CONCLUSIONS

This study was conducted to examine the solar drying characteristics of sugarcane bagasse. One of the world's representative sources of lignocellulose biomass is sugarcane bagasse. In Gwangju, South Korea, an external solar collector-type air heater was constructed to supply the heat energy needed to dry a 900-mm-deep bed of sugarcane bagasse from October 10 to 19th (Fig. 6). In nine days, the average moisture content of sugarcane bagasse decreased from approximately 47%$_{w.b.}$ to

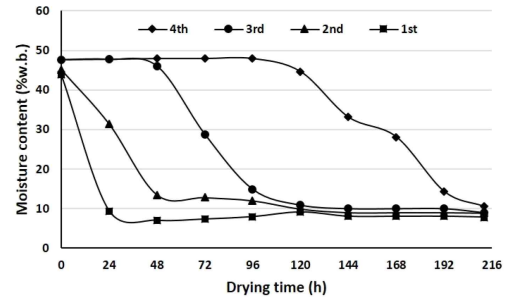

Fig. 6. Solar drying curves of four layers in 900 mm-deep wet sugarcane bagasse fixed bed from October 10th to 19th.

9%$_{w.b}$. It was estimated that 27% of the total solar radiation collected was used to evaporate the water in sugarcane bagasse.

CONFLICT of INTEREST

No potential conflict of interest relevant to this article was reported.

ACKNOWLEDGMENT

This study was supported by the Ministry of Land, Infrastructure and Transport of the Republic of Korea (Project No. 22DPRB-C161884-1).

REFERENCES

Abdel-Rehim, Z.S., Nagib, Z.A. 2007. Solar drying of bagasse pulp. Journal of Applied Sciences Research 3(4): 300-306.

Aisyadea, F., Dewi, G.K., Widyorini, R. 2023. Selected properties of particleboard made from sugar palm (*Arenga pinnata*) dregs. Journal of the Korean Wood Science and Technology 51(5): 334-344.

Akomo, O.J. 2016. Open air drying of bagasse: Potential in sugar industries. M.S. Thesis, University of Nairobi, Kenya.

Arshad, M., Ahmed, S. 2016. Cogeneration through bagasse: A renewable strategy to meet the future energy needs. Renewable and Sustainable Energy Reviews 54: 732-737.

Belessiotis, V., Delyannis, E. 2011. Solar drying. Solar Energy 85(8): 1665-1691.

Cahyani, N., Yunianti, A.D., Suhasman, Pangestu, K.T.P., Pari, G. 2023. Characteristics of bio pellets from spent coffee grounds and pinewood charcoal based on composition and grinding method. Journal of the Korean Wood Science and Technology 51(1): 23-37.

Chabane, F., Moummi, N., Brima, A., Benramache, S. 2013. Thermal efficiency analysis of a single-flow solar air heater with different mass flow rates in a smooth plate. Frontiers in Heat and Mass Transfer 4(1): 013006.

Don, C.E., Mellet, P., Ravno, B.D., Bodger, R. 1977. Calorific values of South African bagasse. In: Mount Edgecombe, South Africa, Proceedings of the South African Sugar Technologists' Association, pp. 169-173.

Dungani, R., Munawar, S.S., Karliati, T., Malik, J., Aditiawati, P., Sulistyono. 2022. Study of characterization of activated carbon from coconut shells on various particle scales as filler agent in composite materials. Journal of the Korean Wood Science and Technology 50(4): 256-271.

El-Sayed, S.A., Mostafa, M.E. 2014. Analysis of grain size statistic and particle size distribution of biomass powders. Waste Biomass Valorization 5: 1005-1018.

Fatriasari, W., Nurhamzah, F., Raniya, R., Laksana, R.P.B., Anita, S.H., Iswanto, A.H., Hermiati, E. 2020. Enzymatic hydrolysis performance of biomass by the addition of a lignin based biosurfactant. Journal of the Korean Wood Science and Technology 48(5): 651-665.

Geldart, D. 1986. Gas Fluidization Technology. John Wiley & Sons, Hoboken, NJ, USA.

Heo, S.J., Choi, J.W. 2017. Study on utilization and prospect of lignocellulosic bioethanol in ASEAN countries. Journal of the Korean Wood Science and Technology 45(5): 588-598.

Iswanto, A.H., Hakim, A.R., Azhar, I., Wirjosentono, B., Prabuningrum, D.S. 2020. The physical, mechanical, and sound absorption properties of sandwich particleboard (SPb). Journal of the Korean Wood Science and Technology 48(1): 32-40.

Jamaludin, M.A., Bahari, S.A., Zakaria, M.N., Saipolbahri, N.S. 2020. Influence of rice straw, bagasse, and their combination on the properties of binderless particleboard. Journal of the Korean

Wood Science and Technology 48(1): 22-31.

Jang, E.S. 2022. Experimental investigation of the sound absorption capability of wood pellets as an eco-friendly material. Journal of the Korean Wood Science and Technology 50(2): 126-133.

Jung, J.Y., Ha, S.Y., Yang, J.K. 2022. Effect of steam explosion condition on the improvement of physico-chemical properties of pine chips for feed additives. Journal of the Korean Wood Science and Technology 50(1): 59-67.

Kim, J., Kim, Y., Jung, S., Yun, H., Yeo, H., Choi, I.G., Kwak, H.W. 2023a. Cationized lignin loaded alginate beads for efficient Cr(VI) removal. Journal of the Korean Wood Science and Technology 51(5): 321-333.

Kim, M.J., Lee, S.J., Kim, S.J., Yang, M.S., Son, D.W., Kim, C.K. 2023b. Study on the combustion characteristics of tulip tree (*Liriodendron tulipifera*) for use as interior building materials. Journal of the Korean Wood Science and Technology 51(5): 410-418.

Kowalczuk, P.B., Drzymala, J. 2016. Physical meaning of the Sauter mean diameter of spherical particulate matter. Particulate Science and Technology 34(6): 645-647.

Krog, W. 2018. Solar live steam generation and solar bagasse drying for South African sugar mills. M.S. Thesis, Stellenbosch University, South Africa.

Kunii, D., Levenspiel, O. 1991. Fluidization Engineering. 2nd ed. Butterworth-Heinemann, Oxford, UK.

Lee, H.W., Eom, C.D. 2021. Preprocessing *Miscanthus sacchariflorus* with combination system of cone grinder and air classifier. Journal of the Korean Wood Science and Technology 49(4): 328-335.

Mohammadi, F., Abdoli, M.A., Amidpour, M., Vahidi, H., Gitipour, S. 2020. Environmental-economic evaluation of sugarcane bagasse gasification power plants versus combined-cycle gas power plants. Global Journal of Environmental Science and Management 6(1): 73-84.

Myeong, S., Lee, Y.J., Kim, D.H., Kim, T.J. 2023. Improvement of inflammation, diabetes, and obesity by forest product-derived polysaccharides through the human intestinal microbiota. Journal of the Korean Wood Science and Technology 51(5): 358-380.

Naeem, N. 2019. Bagasse-based cogeneration in Pakistan: Challenges and opportunities. https://www.bioenergyconsult.com/bagasse-cogeneration-pakistan/

Osborne, N.S., Stimson, H.F., Ginnings, D.C. 1939. Measurements of heat capacity and heat of vaporization of water in the range 0° to 100℃. Journal of Research of the National Bureau of Standards 23: 197-260.

Pari, G., Efiyanti, L., Darmawan, S., Saputra, N.A., Hendra, D., Adam, J., Inkriwang, A., Effendi, R. 2023. Initial ignition time and calorific value enhancement of briquette with added pine resin. Journal of the Korean Wood Science and Technology 51(3): 207-221.

Rasheed, L.A., Mohammed, J.A.K., Jessam, R.A. 2023. Performance enhancement of a single pass solar air heater by adopting wire mesh absorber layer. Joint Journal of Novel Carbon Resource Sciences & Green Asia Strategy 10(2): 880-887.

Saha, S.N. 2020. Thermal performance of single and double exposure solar air heaters. In: Meerut, India, Proceedings of International Conference of Advance Research & Innovation (ICARI) 2020.

Salehi, F.A., Abdoli, M.A., Shokouhmand, H., Jafari, H.R. 2013. Techno-economic assessment for energy generation using bagasse: Case study. International Journal of Energy Research 37(8): 982-990.

Setyayunita, T., Widyorini, R., Marsoem, S.N., Irawati, D. 2022. Effect of different conditions of sodium chloride treatment on the characteristics of kenaf fiber-epoxy composite board. Journal of the Korean Wood Science and Technology 50(2): 93-103.

Shrestha, D. 2022. Nanocomposite electrode materials prepared from *Pinus roxburghii* and hematite for application in supercapacitors. Journal of the Korean Wood Science and Technology 50(4): 219-236.

Struckmann, F. 2008. Analysis of a Flat-plate Solar Collector. Heat and Mass Transport, Lund, Sweden.

Sutapa, J.P.G., Hidyatullah, A.H. 2023. Torrefaction for improving quality of pellets derived from calliandra wood. Journal of the Korean Wood Science and Technology 51(5): 381-391.

Tiwari, G.N. 2002. Solar Energy: Fundamentals, Design Modeling and Applications. CRC Press, Boca Raton, FL, USA.

Zendrato, H.M., Devi, Y.S., Masruchin, N., Wistara, N.J. 2021. Soda pulping of torch ginger stem: Promising source of nonwood-based cellulose. Journal of the Korean Wood Science and Technology 49(4): 287-298.